Reconstruction of two-dimensional phase dynamics from experiments on coupled oscillators

Karen A. Blaha,[1] Arkady Pikovsky,[2] Michael Rosenblum,[2] Matthew T. Clark,[1] Craig G. Rusin,[1] and John L. Hudson[1]
[1]*Department of Chemical Engineering, 102 Engineers' Way, University of Virginia, Charlottesville, Virginia 22904-4741, USA*
[2]*Department of Physics and Astronomy, University of Potsdam, Karl-Liebknecht-Strasse 24/25, D-14476 Potsdam-Golm, Germany*
(Received 21 December 2010; revised manuscript received 1 September 2011; published 4 October 2011)

Phase models are a powerful method to quantify the coupled dynamics of nonlinear oscillators from measured data. We use two phase modeling methods to quantify the dynamics of pairs of coupled electrochemical oscillators, based on the phases of the two oscillators independently and the phase difference, respectively. We discuss the benefits of the two-dimensional approach relative to the one-dimensional approach using phase difference. We quantify the dependence of the coupling functions on the coupling magnitude and coupling time delay. We show differences in synchronization predictions of the two models using a toy model. We show that the two-dimensional approach reveals behavior not detected by the one-dimensional model in a driven experimental oscillator. This approach is broadly applicable to quantify interactions between nonlinear oscillators, especially where intrinsic oscillator sensitivity and coupling evolve with time.

DOI: 10.1103/PhysRevE.84.046201 PACS number(s): 05.45.Tp, 05.45.Xt, 02.50.Sk

I. INTRODUCTION

Systems of coupled oscillators have been investigated in a variety of fields. Examples include coupled lasers [1], population dynamics [2], chemical reactions [3], and cardiorespiratory interactions [4,5], among others. A theoretical description of the system can be obtained in two ways: either write the model equations for the coupled systems starting from the first principles, or reconstruct the model equations from observations. In many cases, e.g., in biological systems, use of the former approach is greatly impeded by underlying complexity and lack of knowledge about oscillation generation and coupling mechanisms.

In this paper we follow the second approach and reconstruct the interaction between a pair of experimental nonlinear electrochemical oscillators. We discuss the basic theory, which we apply for our system of two oscillators with weak coupling. The system is represented in terms of two phases, which in many cases may be simplified to a single variable, the phase difference [6]. We show that phase models that preserve dependence on individual phases generally provide a more detailed description of the interactions between two oscillators than do those based on the phase difference. We compare results of the two modeling methods and discuss limitations of models based on phase difference. We calculate from experimental data a two-phase model using a previously introduced technique [7]. Our results experimentally verify phase reconstruction in a system with noise and connect the two-dimensional and one-dimensional models [6,8,9]. We calculate the natural oscillator frequencies, changes in coupling directionality, and coupling time delay from the experimentally determined phase models. We also present experiments where coupling functions exhibit higher-order terms, and show that these terms are not captured by the one-dimensional model.

II. THEORY

Suppose we observe two interacting oscillators described by

$$\dot{\vec{x}}_i = \vec{F}_i(\vec{x}_i) + \varepsilon \vec{p}_i(\vec{x}_i,\vec{x}_j), \tag{1}$$

where $i = 1,2$, $j = 2,1$, and the parameter ε describes the strength of the interaction. Generally, the functions $\vec{F}_i$ are different; moreover they can be of different dimension. The coupling functions $\vec{p}_i$ can be different as well. We assume that both systems when uncoupled, i.e., when $\varepsilon = 0$, possess stable limit cycles in their phase spaces. The asymptotic dynamics of each oscillator (after transients die out) can be then described by a single variable, the phase [6,9,10].

Even when the equations (1) of the coupled oscillating system are known their analytical treatment can be quite complicated, if at all possible. An essential simplification can be made in the case of weak coupling, where applied perturbations are small compared to the negative Lyapunov exponent(s) of each oscillator. For this case the oscillators remain near their closed orbits and the dynamics of a pair of coupled systems is confined to the two-dimensional torus in the phase space. Correspondingly, the dynamics can be parametrized by two phases [6,9,10],

$$\dot{\phi}_i = \omega_i + Q^{(i)}(\phi_i,\phi_j). \tag{2}$$

Here ϕ_i is the phase of oscillator i, ϕ_j is the phase of the other oscillator, and ω_i is the natural angular frequency of the oscillator i, i.e., the frequency of the uncoupled system. The functions $Q^{(i)}$ describe the coupling between the systems. The only *a priori* assumption about these functions is that they are 2π periodic with respect to both arguments; in particular, they can contain a constant term.

If the dynamical equations (1) are known, the coupling functions $Q^{(i)}$ can be represented in the form of the power series by means of a perturbative expansion [6],

$$Q^{(i)}(\phi_i,\phi_j) = \varepsilon Q_1^{(i)}(\phi_i,\phi_j) + \varepsilon^2 Q_2^{(i)}(\phi_i,\phi_j) + \cdots, \tag{3}$$

where the subscripts on $Q^{(i)}$ correspond to the order of approximation. Computation of the high-order terms represents, to the best of our knowledge, an unsolved problem, whereas the first-order phase approximation is widely used in various applications [6,8]. The first-order coupling functions can be written as

$$Q_1^{(i)}(\phi_i,\phi_j) = \vec{Z}_i(\phi_i) \cdot \vec{h}_i(\phi_i,\phi_j), \tag{4}$$

where $\vec{Z}$ is the phase-dependent response function of the oscillator and $\vec{h} = \vec{p}(\vec{x}_i(\phi_i),\vec{x}_j(\phi_j))$ is the applied stimulation. In the simplest case when the scalar driving is independent of the phase of the driven system and enters the state-space equations (1) as an additive term, the coupling function can be represented as a product of two functions of one variable, $Q_1^{(i)}(\phi_i,\phi_j) = Z_i(\phi_i)h_i(\phi_j)$. The phase description Eq. (2) can be valid for not-so-weak coupling as well: as long as a stable invariant torus in the phase space exists, the motion on it can be parametrized by the phases and the dynamics can be written in the form of Eq. (2).

A large body of work concerns the description of two interacting oscillators as a function of the phase difference [11]. Theoretical studies and numerical simulations show that these one-dimensional phase models capture the important synchronization properties of populations of similar oscillators with weak interactions [12–18]. Phase difference based phase models also predict system behavior in electrochemical experiments [19]. The one-dimensional approach is suitable, because the long-term dynamical effects, such as synchronization, depend mainly on the averaged coupling functions q, discussed below.

The reduction to a one-dimensional description can be made if the coupling is also weak compared to the natural frequency, i.e., the norm of the coupling function $||Q^{(i)}|| \ll \omega_i$, and the natural frequencies of two systems are close to a resonance condition, $m\omega_1 \approx n\omega_2$. In this case one can introduce a slow variable, phase difference,

$$\psi = n\phi_2 - m\phi_1,$$

and average Eq. (2) over the common oscillation period $T = 2\pi n/\omega_1 \approx 2\pi m/\omega_2$. In the case of similar oscillators ($m = n = 1$), ψ reduces to $\phi_2 - \phi_1$. The averaged equations have the form [6]

$$\dot{\phi}_i = \omega_i + q_{m,n}^{(i)}(\psi), \tag{5}$$

where the new, averaged coupling function $q_{m,n}$ is a function of the phase difference only,

$$q_{m,n}^{(i)}(\psi) = \frac{\varepsilon}{2\pi}\int_0^{2\pi} Q^{(i)}\left(\phi_1, \frac{m}{n}\phi_1 + \frac{\psi}{n}\right) d\phi_1. \tag{6}$$

Thus, a description in terms of phase difference is possible only in vicinities of the resonant frequency ratios. For each of the resonant tongues one should establish an averaged coupling function $q_{m,n}$. Thus, although a complete description of the coupled system for any frequency ratio can be achieved with one pair of two-dimensional functions Q, a large set of one-dimensional coupling functions is required to provide the same result.

We illustrate the difference in synchronization predictions between two- and one-dimensional phase models by an analysis of the following toy model of a harmonically driven oscillator:

$$\dot{\phi}_1 = \omega_1 + \varepsilon[\cos(\phi_1) + \cos(2\phi_1)]\sin(\phi_2), \tag{7}$$

$$[2ex]\dot{\phi}_2 = \omega_2. \tag{8}$$

Averaging Eq. (7) using Eq. (6) yields two nontrivial one-dimensional coupling functions $q_{1,1} = \frac{\varepsilon}{2}\sin(\phi_2 - \phi_1)$ and $q_{2,1} = \frac{\varepsilon}{2}\sin(\phi_2 - 2\phi_1)$; all other functions $q_{n,m} = 0$. Thus, the averaged description of Eq. (7) predicts locking only when $\omega_1 \approx \omega_2$ and $2\omega_1 \approx \omega_2$, with triangular Arnold tongues. However, the tongues obtained by numerical simulation of the full model (7) differ from the triangular shape when ω_2 is farther from the resonance frequencies, as shown in Figs. 1(a) and 1(b). Furthermore, numerical analysis of Eq. (7) shows many locking regions, as seen in Fig. 1(c), in contrast to predictions of the reduced model. We explore the applications of the two-dimensional method and compare the one- and two-dimensional methods in the following sections.

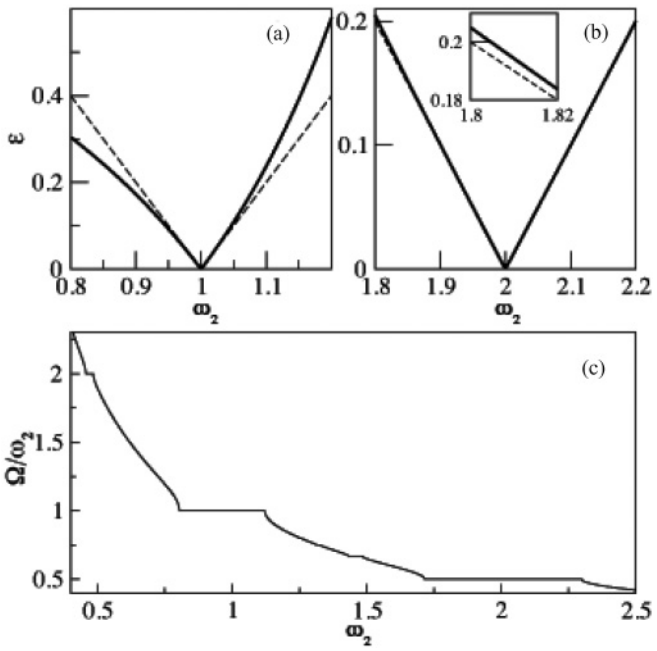

FIG. 1. (a) Main synchronization tongue for the two-dimensional model Eq. (7) (solid line) and the tongue predicted by the one-dimensional model $q_{1,1}$ (dashed line). (b) The second tongue at $\omega_2 \approx 2$ for the two-dimensional model (solid line) and for the one-dimensional model $q_{2,1}$ (dashed line). Here the averaging works well and the difference is pronounced only far from resonance (see inset). (c) Devil's staircase for the toy model Eq. (7) with $\omega_1 = 1$, for $\varepsilon = 0.3$; here $\Omega = \langle\dot{\phi}\rangle$ where $\langle\cdot\rangle$ is time average. Locking regions at $\Omega/\omega_2 = 2$, $\Omega/\omega_2 = 1$, $\Omega/\omega_2 = 2/3$, and $\Omega/\omega_2 = 1/2$ are seen. Zoom of the plot (not shown) exhibits further locking ratios, e.g., 3/2, 4/5, 3/4, and 3/5.

III. EXPERIMENTAL SETUP

Experiments were performed on an electrochemical cell consisting of two Ni working electrodes (99.98% pure), a Pt mesh counterelectrode, and $Hg/Hg_2SO_4/K_2SO_4$ (sat) reference electrode, with a $3M$ H_2SO_4 electrolyte, shown in Fig. 2(a). The cell was enclosed in a jacketed glass vessel maintained at a temperature of 11 °C. An ACM Instruments multichannel potentiostat was used to individually set the electrode potential V_i of each electrode such that the electrodes undergo transpassive dissolution.

A 650 Ω resistor was attached to each electrode, causing the dissolution current to oscillate [20]. The resulting dissolution currents were measured using a zero resistance ammeter attached to a real-time data acquisition system, Fig. 2(a). The

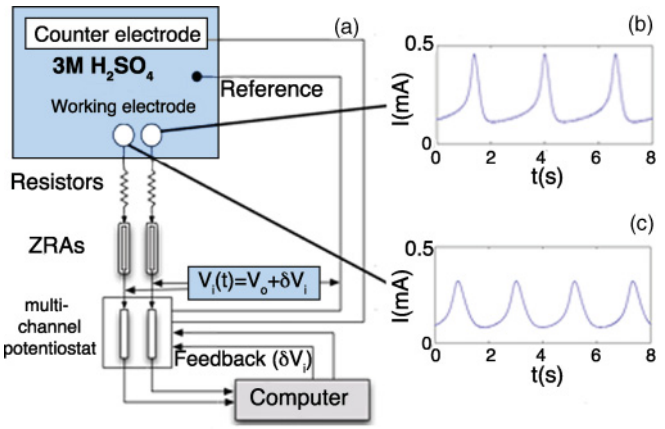

FIG. 2. (Color online) (a) Experimental apparatus with multichannel addressable voltage and feedback. (b) Time series of relaxational oscillations at $V = 1.210$ V. (c) Electrochemical dissolution time series showing smooth oscillations at a potential of $V = 1.105$ V, ZRA: zero resistance ammeter.

shape of the electrochemical oscillator wave form depends on applied voltage. Smooth oscillations with a natural frequency of about 0.5 Hz are observed at potentials of approximately 1.105 V. Relaxational oscillations with a frequency of about 0.35 Hz are observed around 1.20 V [21]. As the applied voltage of each electrode in the experimental system can be chosen independently, any combination of smooth or relaxation oscillators is accessible. Relaxational and smooth oscillations are shown in Figs. 2(b) and 2(c), respectively. Here, oscillator 1 refers to the more relaxational oscillator ($V_1 = 1.180$ V) with a natural frequency of $\nu_1 = 0.405$ Hz $\pm$ 0.005 Hz, while oscillator 2 ($V_2 = 1.105$ V) refers to the smooth oscillator with a natural frequency of $\nu_2 = 0.479$ Hz $\pm$ 0.002 Hz, where $\nu = \omega/2\pi$. The range is due to the slow drift over time of the natural frequencies of the oscillators as an inherent property of the system.

Negligible intrinsic electrical interactions exist between the uncoupled oscillators. The startup or shutdown of an oscillator does not alter the behavior of the second oscillator. Furthermore, the oscillator dynamics have no interdependence when both oscillators are functioning in the uncoupled state.

Interactions were introduced using real-time coupling of the form

$$\Delta V_1(t) = K[k_1 x_2(t-\tau)], \tag{9}$$

$$[2ex]\Delta V_2(t) = K[k_2 x_1(t-\tau)], \tag{10}$$

where $\Delta V_{1,2}$ are the changes in the circuit potentials of the elements, K is the fixed overall coupling gain, k_1 and k_2 are the coupling gains on oscillator 1 and oscillator 2, respectively, such that $0 \leqslant k_i \leqslant 1$, and τ is the coupling time delay. The scaled potentials of the elements as a function of time $x_i(t)$ are

$$x_i(t) = V_i(t) - I_i(t)R_p, \tag{11}$$

where V_i are the applied potentials, I_i are the normalized currents, and $R_p = 650\ \Omega$ is the channel resistance. Only linear coupling is considered here, with and without time delay [22,23].

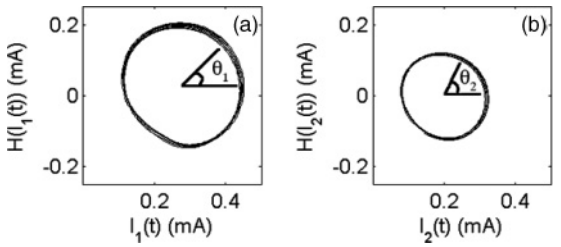

FIG. 3. Time series in Hilbert space; θ_i indicates protophase (a) for the relaxational oscillator and (b) for the smooth oscillator. Note that although the phase portraits look very much alike, the distributions of θ_i are different, as shown in Fig. 4(b).

IV. METHODS

The only information required by the phase models in Eqs. (2) and (5) is the instantaneous phases. The instantaneous phases are calculated directly from the electrochemical current time series using the phase space angle, as shown in Fig. 3. Other definitions of phase are equally applicable provided they yield a one-to-one correspondence between phase and location on the closed orbit [8,24,25]. For example, phase defined from the percentage of trajectory length between consecutive Poincaré surface of section crossings is useful for more complicated oscillations (e.g., electrocardiograms) [7].

Electrodissolution currents of each element are measured at 250 Hz, filtered with a 129 point fourth-order Savitsky-Golay filter, and used to calculate the genuine phases. The Savitsky-Golay filter preserves the structure of the oscillation while removing nonphysical phase velocities caused by noise in the system. Although the maximum amplitude of the relaxation oscillator (oscillator 1) tends to be underestimated, the phase is well preserved; the difference between the phases calculated from filtered and unfiltered signals is delta correlated.

Note that definitions of phase based on the Hilbert transform have inherent deviations in phase velocity as a function of phase. These deviations arise from the nonsinusoidal nature of the oscillations. This introduces strong dependence on phase into oscillator phase velocity in the absence of perturbations. Such a dependence contradicts the definition of phase lying at the basis of Eq. (2), as in this equation phase increases uniformly in the absence of interactions. Moreover, this dependence swamps the effect of perturbations on the instantaneous rate of phase advance [see Fig. 4(a)]. These phases obtained directly from the embeddings in Fig. 3 are thus referred to as θ, the protophases. In order to isolate phase velocity changes resulting from perturbations, phase must be defined as increasing linearly in the absence of perturbations. A nearly linearly increasing phase is obtained with the help of the protophase probability density distribution $(2\pi)^{-1}\sigma(\theta_i)$ [7], which is the inverse of the average instantaneous velocity of the oscillator through the limit cycle [see Fig. 4(b)]. The genuine phases ϕ result from the transformations $d\phi_i/d\theta_i = \sigma(\theta_i)$, and exhibit nonlinear phase advance in response to coupling or feedback only. This is evident in Fig. 4(c), where the overall phase advance is uniform while localized excursions remain.

From the transformed, genuine phases ϕ_i we find the coupling functions Q, following the methods of [7]. First, the phase of each oscillator is cleansed of nonuniform

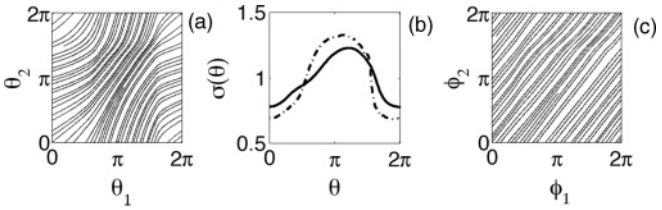

FIG. 4. (a) Wrapped protophase of oscillator 1 (relaxational, $V_1 = 1.180$ V) versus protophase of oscillator 2 (smooth, $V_2 = 1.105$ V) obtained via the Hilbert transform. (b) Phase transformation function, σ. $\sigma(\theta_1)$ is dash-dotted, and $\sigma(\theta_2)$ is solid. (c) Wrapped genuine phases of the two oscillators, ϕ_1 and ϕ_2.

phase advance. Then the phase velocities are fit with a two-dimensional Fourier expansion, Eq. (18) in [7] (when the phase space is not well covered, phase velocities are instead fit with a two-dimensional kerneling function). The coupling functions are then further cleansed using the method in Sec. IV, part B in [7]. Numerics demonstrate that satisfactory results can be obtained already after the first cleansing, since the second cleansing is small compared to the first. Note two limitations of the method (see [7] for details): (i) if the coupling function contains a component dependent only on the phase of the driven system, it will be cleansed; and (ii) generally the coupling function contains a constant term which cannot be separated from the natural frequency; this may be done only if several observations with different yet unknown coupling strengths are available. A MATLAB implementation of the techniques employed for the data analysis may be found online [26].

There is more than one way to obtain the one-dimensional coupling functions, $q^{(i)}$. These can be obtained as in Eq. (6), by averaging from the two-dimensional coupling functions $Q^{(i)}$, or they can be obtained directly from the time series [3]. The methods are conceptually equivalent, and yield nearly identical results. The latter is easier to implement numerically, and we use it here to obtain $q^{(i)}$. First, the periods of each oscillation are calculated. The inverse of the period is the average frequency over the oscillation. Next, we calculate the average phase difference over each oscillation. Here we express phase difference as obtained from the genuine phases; phase differences from the protophases distort the coupling function if the oscillators are dissimilar. Finally, $q^{(i)}$ is obtained by fitting the average frequency as a function of phase difference. The fitting can be performed with a Fourier series or a kerneling function.

V. RESULTS

Experiments were performed using the two-oscillator electrochemical system described in Sec. III. Oscillator 1 has a relaxational wave form ($V_1 = 1.180$ V) and oscillator 2 has a smooth wave form ($V_2 = 1.105$ V). The oscillators are coupled using the form in Eqs. (9) and (10). Phase models of the two oscillators are then reconstructed from the genuine phase time series according to Eq. (2) or the procedure for the one-dimensional reconstruction discussed in Sec. IV.

In order to highlight the advantages of the two-dimensional coupling function, we compare the coupling functions of the one- and two-dimensional models with symmetrical

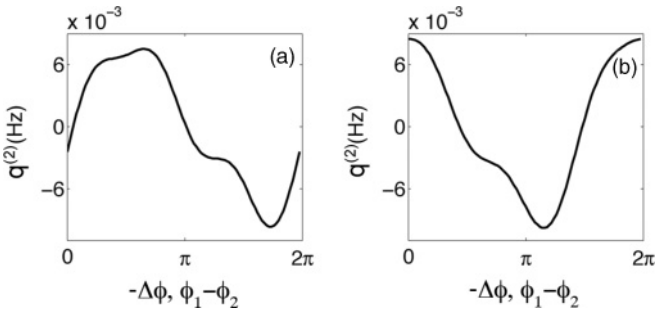

FIG. 5. Coupling function for oscillator 2 based on phase difference, $q^{(2)}(\phi_1 - \phi_2)$. (a) No time delay, $\tau = 0$. (b) Time delay equal to roughly three-quarters of oscillator 2 natural period, $\tau = 1.8$ s.

coupling with and without time delay. Figure 5(a) shows the one-dimensional coupling function of oscillator 2 based on phase difference. The phase model of oscillator 1 is obtained in a similar fashion, but is not shown. This coupling function quantifies the oscillator's average change in frequency over a period. For example, when $\Delta\phi = \pi/2$ the frequency of oscillator 2 increases relative to its natural frequency. Figure 6(a) shows the two-dimensional coupling function of oscillator 2 based on each phase independently. The one-dimensional phase model, Fig. 5(a), is the average of this two-dimensional model over trajectories between two crossings of $\phi_2 = 0$, i.e., one period. Note that the amplitude of the one-dimensional coupling function is an order of magnitude smaller than the two-dimensional due to the averaging. The two-dimensional function provides a mapping between instantaneous changes in phase velocity and the state of each system. For example, oscillator 2 advances most rapidly near $\phi_1 = \pi/2$ and $\phi_2 = 3\pi/2$.

Further experiments were performed in order to quantify the effects of time delay. From the definitions of the coupling function in Eqs. (4) and (6), time delay is expected to shift the stimulation function in the phase of the perturbing oscillator. Figure 5(b) shows the coupling function of oscillator 2 based on phase difference for symmetric coupling and time delay of $\tau = 1.8$ s. The phase model based on individual phases for this case is shown in Fig. 6(b). Notice that both coupling functions are translated as expected. However, the two-dimensional coupling function clearly distinguishes between shifts in the two phases: Fig. 6(b) becomes nearly identical to Fig. 6(a)

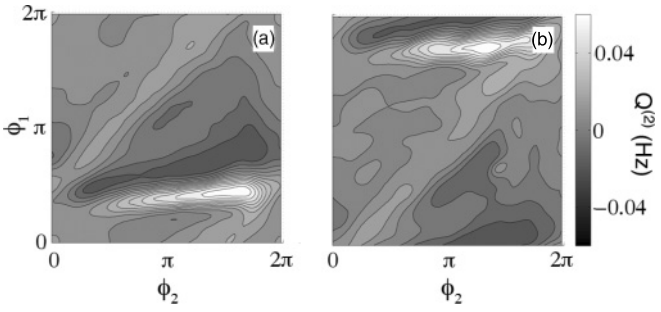

FIG. 6. Coupling function in Hz for oscillator 2 based on each phase independently, $Q^{(2)}(\phi_2,\phi_1)$. (a) No time delay, $\tau = 0$. (b) Time delay equal to three-quarters the natural period of oscillator 2, $\tau = 1.8$ s.

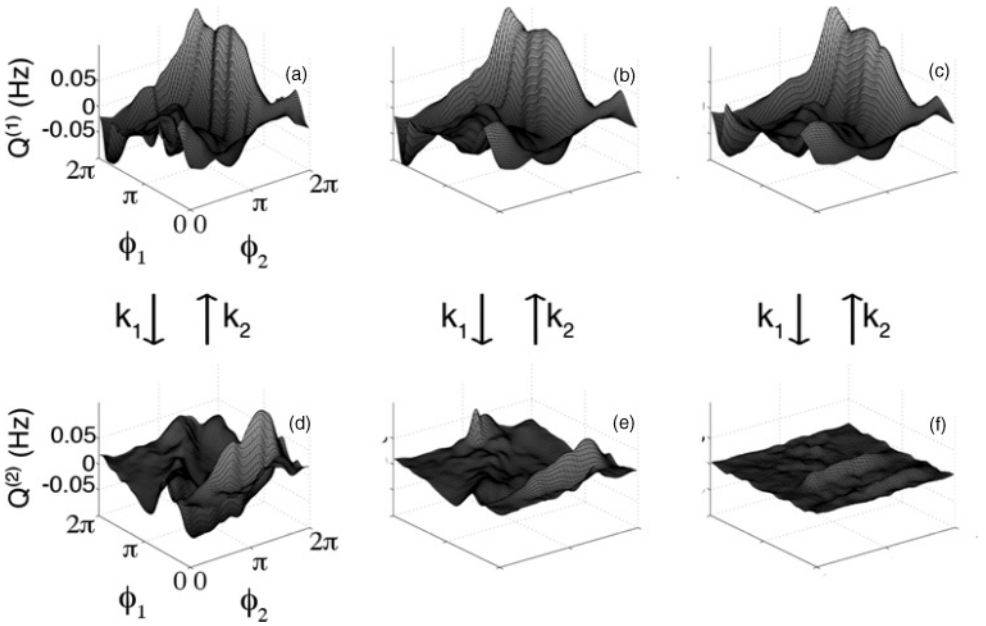

FIG. 7. (Top row) $Q^{(1)}(\phi_1,\phi_2)$; (bottom row) $Q^{(2)}(\phi_2,\phi_1)$. $k_2 = 1.0$ for all plots. [(a), (d)] $k_1 = 1.0$, [(b), (e)] $k_1 = 0.5$, and [(c), (f)] $k_1 = 0.1$.

if one shifts the phase of the forcing oscillators ϕ_1 by $\tau\nu_1 2\pi = 4.58$ rad. Therefore, changes in coupling time delay are measurable from the two-dimensional model to within an additive factor of 2π. Time delay may be recovered from the one-dimensional model provided that the response function is known to be time invariant.

Now we investigate the effect of changing coupling magnitude on the phase models. Focus is placed on the two-dimensional model, as it provides a more complete description of the system. Oscillator 1 is a relaxational oscillator ($V_1 = 1.210$ V) with a natural frequency of 0.42 Hz $\pm$ 0.02 Hz and oscillator 2 is a smooth oscillator ($V_2 = 1.105$ V) with a natural frequency of 0.53 Hz $\pm$ 0.01 Hz. Figure 7 shows the coupling functions of oscillators 1 and 2 as a function of the genuine phases. The means of the coupling functions are less than 1% of the natural frequency, indicating a negligible change in average frequency due to coupling. Three coupling combinations (k_1:k_2) are shown: symmetric, asymmetric (1:2), and highly asymmetric (1:10). As expected from Eq. (4), the amplitude of the surface variations decreases with diminishing stimulation magnitude. Also note that the functional dependence of each coupling function on its own phase is characteristic of the oscillator's response function [19].

The magnitude of an oscillator's response is quantified by the L_2 norm of its coupling function, Q. Figure 8 shows the dependence of the coupling function norms on the coupling strengths k_1 and k_2. In this series of experiments the coupling strength to oscillator 2 was held constant at $k_2 = 1.0$, while the strength of the coupling to oscillator 1, k_1, was increased incrementally from zero to 1.0. In a subsequent series of experiments with the same oscillators, the coupling strength on oscillator 1 was held constant at $k_1 = 1.0$ and k_2 was decremented from 1.0 to zero. Figure 8 shows that the norm of the coupling function increases linearly with increasing coupling strength. This experimentally confirms that the coupling of electrochemical oscillators in the range of parameters studied is predominantly described by first-order terms in the coupling strength, i.e., we are in the regime of linear response.

The relative magnitudes of the coupling functions indicate the coupling directionality between the oscillators. In the electrochemical system described above, the values of k_1 and k_2, and therefore the relative coupling magnitude, are known from the experimental setup. The applied directionality is

$$d_A = \frac{k_1 - k_2}{k_1 + k_2}. \tag{12}$$

Thus, d_A varies between -1 and 1. The more positive the directionality, the stronger k_1 is relative to k_2. A directionality of zero indicates equal coupling strengths, i.e., $k_1 = k_2$. We can compare this quantity with the *observed directionality*, defined as

$$d_O = \frac{C_1 - C_2}{C_1 + C_2}, \tag{13}$$

where $C_i = ||Q^{(i)}||/\omega_i$. As shown in Fig. 8, the relaxational oscillator has a greater response to the same coupling gain and thus less voltage perturbation, according to Eq. (9). Therefore d_A and d_O are generally different. When the norms are scaled

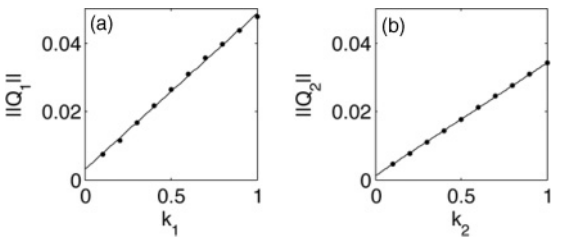

FIG. 8. (a) Relaxational oscillator: Norm versus gain k_1, linear fit: $||Q^{(1)}|| = 0.045k_1 + 0.003$, $R^2 = 0.998$. (b) Smooth oscillator: Norm versus gain k_2, linear fit: $||Q^{(2)}|| = 0.032\ k_2 + 0.001$, $R^2 = 1.000$, where R^2 is the square of the correlation coefficient.

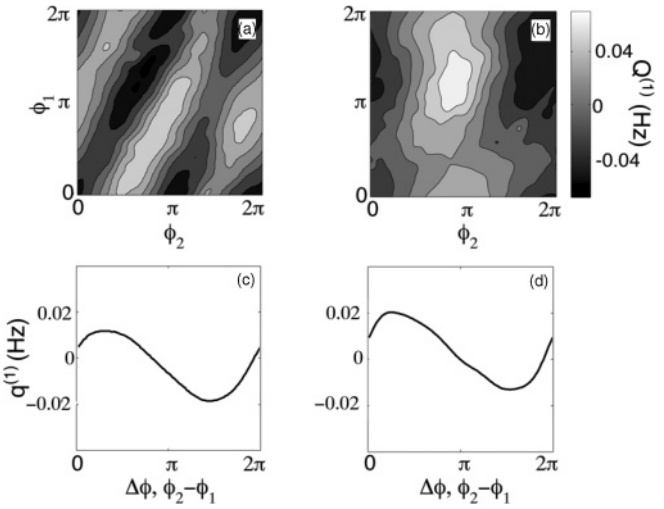

FIG. 9. Experimental results: (a) $Q^{(1)}$ with $\nu/\omega = 0.95$, (b) $Q^{(1)}$ with $\nu/\omega = 1.05$, (c) $q^{(1)}_{1,1}$ with $\nu/\omega = 0.95$, and (d) $q^{(1)}_{1,1}$ with $\nu/\omega = 1.05$.

by the response slope from Fig. 8, one restores $d_O = d_A$. Here we know $k_{1,2}$ and thus can obtain the response slopes; in general, $k_{1,2}$ may not be known.

Next we carried out experiments on an electrochemical oscillator with adjustable harmonic forcing. Figure 9 shows the coupling functions, $Q^{(1)}$ and $q^{(1)}$, when the forcing frequency is 5% faster [(a) and (c)], and when the forcing frequency is 5% slower [(b) and (d)] than the natural frequency of the oscillator for a smooth ($V = 1.105$ V) oscillator. We see that the two-dimensional coupling function varies with forcing frequency, while the change is not detectable in the one-dimensional coupling function. The observed dependence of the two-dimensional coupling functions on the frequency of the driving has also been observed numerically with the harmonically forced van der Pol and periodic Rössler oscillators.

VI. DISCUSSION

In this paper we evaluate the coupling functions for two coupled nonlinear electrochemical oscillators directly from measured signals. We evaluate both the one- [3,29] and two-dimensional [7] coupling functions and compare the results of the models. While both models may recover changes in coupling time delay, only the two-dimensional model clearly distinguishes between changes in oscillator character and changes in time delay. We show that the relative magnitudes of the coupling functions quantify the directionality of coupling [27,28]. Using a toy model we show that the two-dimensional model predicts more synchronization regions and predicts the synchronization gain more accurately than the one-dimensional model. With an experimental oscillator driven by a harmonic voltage perturbation, we show that the two-dimensional model captures changes in the coupling function that are not detected by the one-dimensional coupling function.

We changed the coupling time delay and calculated the one- and two-dimensional coupling functions (Figs. 5 and 6). The two-dimensional function indicates the precise configurations of *both* phases that correspond to maximum and minimum phase advance. Phase models based on generalized phase difference average out dependence of phase advance on the individual phases. Therefore in a one-dimensional coupling function, a shift may be due to changes in time delay or in oscillator characteristics. Systems where the coupling and intrinsic system properties evolve with time include physiological and medical applications. Unless the oscillator is known to be time invariant, the two-dimensional coupling function is the preferable model for inferring time delay.

We performed experiments in which we varied the ratio of the coupling components, k_1 and k_2 in Eqs. (9) and (10). We then calculated the two-dimensional coupling functions. Deviations from linear phase advance indicate points in phase space where an oscillator is susceptible to perturbation and is stimulated. This is nicely visualized in the top row of Fig. 7 which shows the instantaneous frequencies of the relaxational oscillator. There is a dominant ridge in the middle of the surface corresponding to maximum amplitude of the smooth oscillator, and therefore the greatest stimulation. A similar result is seen for the smooth oscillator in Fig. 7(c). The largest instantaneous frequency on the ridge occurs near $\phi_1 = 3\pi/2$, which corresponds to the large amplitude in the oscillator phase-dependent response curve [19]. From the coupling functions, the coupling directionality was calculated, as in Eq. (13). The nearly linear increase in the norms of the coupling functions with gain, shown in Fig. 8, is a verification of the two-dimensional reconstruction.

Using the toy model of Eq. (7), we highlight the differences of the predictions of the one- and two-dimensional models. We construct two Arnold tongues, and show that the synchronization gains predicted by the two models differ increasingly as the forcing frequency becomes farther from the resonance condition. Additionally, we show that the two-dimensional model predicts many regions of synchrony in a Devil's staircase; the one-dimensional model predicts only two regions of synchrony. The differences between the predictions of the two models in a relatively simple and explicitly defined system illustrate how the two models may differ in more complex systems.

Finally, we show from experimental data that the two-dimensional coupling function depends upon the forcing frequency, while the one-dimensional coupling function does not (Fig. 9). As already mentioned, the phase approximation is valid if the cycle is sufficiently stable and therefore the amplitudes can be considered as fixed. For this case the coupling function $Q^{(i)}$ can be reconstructed from data. If the coupling is sufficiently small, this function can be approximated by only one term of the series equation (3), i.e., $Q^{(i)}(\phi_i,\phi_j) \approx \varepsilon Q^{(i)}_1(\phi_i,\phi_j)$, and in this approximation the function depends solely on the phases, but not on the frequencies. However, the condition when the first approximation suffices is not yet known, and if it is not fulfilled, we can expect a dependence on the frequency and on the amplitude of the forcing. In this experiment, neither the stimulation function nor the response function changes, so we may infer according to Eq. (4) that the first-order approximation does not hold. The effect of forcing frequency on the coupling function

was not previously predicted or shown; this effect as well as the range of applicability of the first-order approximation represent opportunities for further study.

An interesting and practically important problem is determination of the response function $Z_i(\phi_i)$ from the observation of the driven system. The ability to separate stimulation and response could be useful in any system where coupling evolves over time, such as systems where learning occurs [30,31]. When the first-order approximation is valid, as in Eq. (4), the coupling function can be represented as a product $Q_1^{(i)}(\phi_i,\phi_j) = Z_i(\phi_i)h_i(\phi_j)$. Because there is indication of significant higher-order terms in the coupling function, the first-order approximation is not valid here and the deconvolution is not possible. We can suggest an alternative explanation for this; the driving may enter the state-space equations (1) as a multiplicative term, e.g., as $f(x_1)g(\nu t)$; in the process of phase reduction this term yields a function of two phases which cannot be written as a product of two one-dimensional functions. This important issue also requires further studies.

ACKNOWLEDGMENT

This work was supported in part by the National Science Foundation (CBET-0730597).

[1] A. M. Yacomotti, G. B. Mindlin, M. Giudici, S. Balle, S. Barland, and J. Tredicce, Phys. Rev. E **66**, 036227 (2002).
[2] B. Blasius, A. Huppert, and L. Stone, Nature (London) **399**, 354 (1999).
[3] J. Miyazaki and S. Kinoshita, Phys. Rev. Lett. **96**, 194101 (2006).
[4] M. G. Rosenblum, L. Cimponeriu, A. Bezerianos, A. Patzak, and R. Mrowka, Phys. Rev. E **65**, 041909 (2002).
[5] R. Mrowka, L. Cimponeriu, A. Patzak, and M. G. Rosenblum, Am. J. Physiol. Regulatory Integrative Comp. Physiol. **285**, R1395 (2003).
[6] Y. Kuramoto, *Chemical Oscillations, Waves and Turbulence* (Springer, Berlin, 1984).
[7] B. Kralemann, L. Cimponeriu, M. Rosenblum, A. Pikovsky, and R. Mrowka, Phys. Rev. E **77**, 066205 (2008).
[8] A. Pikovsky, M. Rosenblum, and J. Kurths, *Synchronization: A Universal Concept in Nonlinear Sciences* (Cambridge University Press, Cambridge, 2001).
[9] A. T. Winfree, *The Geometry of Biological Time* (Springer-Verlag, Berlin, 1980).
[10] A. T. Winfree, J. Theor. Biol. **16**, 15 (1967).
[11] J. A. Acebron, L. L. Bonilla, C. J. P. Vicente, F. Ritort, and R. Spigler, Rev. Mod. Phys. **77**, 137 (2005).
[12] H. Sakaguchi, S. Shinomoto, and Y. Kuramoto, Prog. Theor. Phys. **77**, 1005 (1987).
[13] G. B. Ermentrout and N. Kopell, J. Math. Biol. **29**, 195 (1991).
[14] D. Hansel, G. Mato, and C. Meunier, Phys. Rev. E **48**, 3470 (1993).
[15] K. Okuda, Physica D **63**, 424 (1993).
[16] S. K. Han, C. Kurrer, and Y. Kuramoto, Phys. Rev. Lett. **75**, 3190 (1995).
[17] H. Daido, Physica D **91**, 24 (1996).
[18] S. H. Strogatz, Physica D **143**, 1 (2000).
[19] I. Z. Kiss, Y. Zhai, and J. L. Hudson, Phys. Rev. Lett. **94**, 248301 (2005).
[20] D. Haim, O. Lev, L. M. Pismen, and M. Sheintuch, J. Phys. Chem. **96**, 2676 (1992).
[21] Y. Zhai, I. Z. Kiss, and J. L. Hudson, Phys. Rev. E **69**, 026208 (2004).
[22] M. K. Stephen Yeung and S. H. Strogatz, Phys. Rev. Lett. **82**, 648 (1999).
[23] E. Montbrió, D. Pazó, and J. Schmidt, Phys. Rev. E **74**, 056201 (2006).
[24] E. Rodriguez, N. George, J. P. Lachaux, J. Martinerie, B. Renault, and F. J. Varela, Nature (London) **397**, 430 (1999).
[25] D. J. DeShazer, R. Breban, E. Ott, and R. Roy, Phys. Rev. Lett. **87**, 044101 (2001).
[26] B. Kralemann, M. Rosenblum, and A. Pikovsky, On-line toolbox, see www.agnld.uni-potsdam.de/∼mros/damoco.html.
[27] M. G. Rosenblum and A. S. Pikovsky, Phys. Rev. E **64**, 045202(R) (2001).
[28] B. Bezruchko, V. Ponomarenko, M. G. Rosenblum, and A. S. Pikovsky, Chaos **13**, 179 (2003).
[29] I. Z. Kiss, C. G. Rusin, H. Kori, and J. L. Hudson, Science **316**, 1886 (2007).
[30] M. A. Trevisan, S. Bouzat, I. Samengo, and G. B. Mindlin, Phys. Rev. E **72**, 011907 (2005).
[31] P. Seliger, S. C. Young, and L. S. Tsimring, Phys. Rev. E **65**, 041906 (2002).